Int. J. Heat Mass Transfer. Vol. 23, pp. 269–278.

0017-9310/80/0301-0269 $02.00/0

BUOYANCY DRIVEN FLOWS ORIGINATING FROM HEATED CYLINDERS SUBMERGED IN A FINITE WATER LAYER

F. P. INCROPERA and M. A. YAGHOUBI
Heat Transfer Laboratory, School of Mechanical Engineering,
Purdue University, West Lafayette, IN 47907, U.S.A.

(*Received* 22 *March* 1979 *and in revised form* 25 *June* 1979)

Abstract – Flow visualization and temperature measurements are used to study conditions in shallow water layers heated from below by cylindrical sources and cooled from above by an air interface. Experiments have been performed for a single horizontal cylinder and for an array of five cylinders, with Rayleigh numbers in the range from 10^5 to 10^6. The free convection boundary layer which develops on the cylinders is laminar, and boundary layer merger occurs at the top of the cylinders without separation. Although the plume which rises above the single cylinder is laminar, its interaction with the air interface produces a horizontal turbulent mixing layer in which vortex rings are formed and penetrate into the underlying fluid. The interaction of plumes generated by the array of cylinders occurs in different ways, depending upon the height ratio.

NOMENCLATURE

D, cylinder diameter [mm];
d_1, distance from bottom of cylinder to bottom of test cell [mm];
g, acceleration due to gravity [m s^{-2}];
H, test cell height [mm];
H_1, water layer depth [mm];
Ra_D, Rayleigh number, $\dfrac{g\beta D^3(T_c - T_w)}{\nu\alpha}$;
T, temperature;
W, test cell width [mm].

Greek symbols

α, thermal diffusivity [m^2 s^{-1}];
β, volumetric coefficient of thermal expansion [K^{-1}];
ν, kinematic viscosity [m^2 s^{-1}].

Subscripts

a–w, air–water interface;
c, cylinder surface condition;
w, bulk water condition.

INTRODUCTION

BUOYANCY driven flows due to distributed heat sources submerged in bounded quiescent liquids exist when oil is preheated in a storage tank, waste heat is dissipated in a closed-cycle cooling system, or when a sensible energy storage system is being charged. Flow conditions can strongly influence heat transfer from the source to the liquid and hence the thermal performance of the system. This study is concerned with buoyancy induced flows which result when one or more heated, horizontal cylinders are submerged in a finite water layer having an air–water interface. For the configuration of Fig. 1, flow originates with a free convection boundary layer which merges at the top of the cylinder to form a two-dimensional plume. The plume is deflected by the air–water interface and subsequently cools due to heat transfer to the surroundings and the entrainment of underlying fluid. Hence a recirculation pattern is induced in which warm water rises with the plume, is cooled at the free surface, and descends along the side boundaries. For an array of cylinders, plumes generated by adjoining

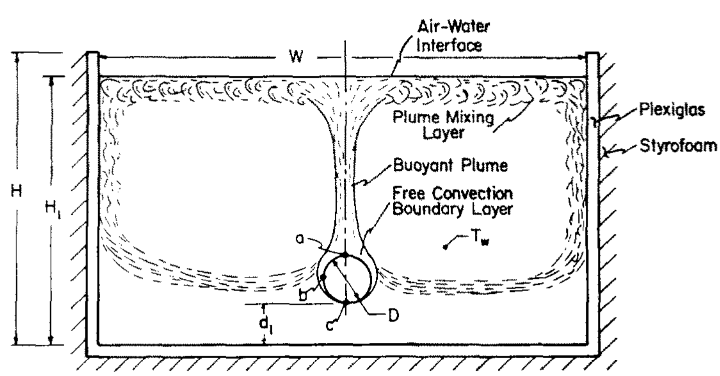

FIG. 1. Schematic of flow in a shallow water layer with a submerged heated cylinder.

cylinders may interact with each other, before or after interacting with the interface, complicating the nature of the recirculation pattern.

Previous studies of natural convection due to distributed heat sources in an extensive fluid have focused on plume development above line sources or boundary layer development on cylinders and spheres. Forstrom and Sparrow [1] and Fujii *et al.* [2] studied the laminar, buoyant plume rising above a single horizontal line source in air, water and spindle oil and have observed a slow, regular swaying motion. Lieberman and Gebhart [3] and Pera and Gebhart [4] observed the mutual interaction and the interaction with adjoining surfaces of plumes rising from an array of line sources in air, while Skipper *et al.* [5] observed no swaying motion or interaction between plumes rising from horizontal cylinders submerged in fuel oil. Pera and Gebhart [6] observed boundary layer and plume conditions near the top of a submerged cylinder, while Eichorn *et al.* [7] studied plume development above spheres and cylinders immersed in a stratified water layer.

Despite the contributions of the foregoing studies, much remains to be learned concerning plume development, interaction and recirculation in finite media, particularly in liquids having an air interface. In this work flow visualization and temperature measurements are used to study the buoyancy induced motion due to a single horizontal cylinder and an array of cylinders in water layers having finite boundaries and an air interface. Emphasis is placed on boundary layer motion around the cylinders, plume development above the cylinders, and the interaction of plumes with each other and the air interface.

EXPERIMENTAL METHODS

Experiments were performed using the test cell shown in Fig. 1. The cell was constructed from Plexiglas and insulated on the bottom and sides with Styrofoam. Its width W and length L (along the cylinder axis) were fixed at 280 and 225 mm, respectively, and machined copper cylinders of outside diameter D = 25.4 mm were installed at a fixed distance of d_1 = 25.4 mm from the bottom. Experiments were performed for a single cylinder installed midway along the width and for an array of five cylinders installed on 50.8 mm centers. For the flow visualization studies the test cell height was initially H = 140 mm and was varied by sacrificing the cell. That is, with completion of the experiments for one value of H, a top section of the cell was removed, and the experiments were repeated. Height ratios in the range $2.5 \leq (H_1/D) \leq 5.0$ were considered, and in all of the experiments the air–water interface was maintained at a fixed distance of $(H - H_1)$ = 12.7 mm from the top of the cell.

The cylinders were drilled to permit the insertion of electrical heaters, and the midplane ($L/2$) surface temperature was measured at three locations on the circumference (points a, b and c of Fig. 1), with the results varying by less than 0.5°C. Temperature control was maintained automatically for the single cylinder and for the central cylinder of the array by wiring the thermocouple at point c to a power controller. Power to the remaining cylinders of the array was manually and independently controlled, and it was possible to maintain the five cylinder surface temperatures to within 0.15°C of each other. Surface temperature measurements were also made along the axial direction of selected cylinders, and in no case did the variation from the midplane to the end exceed 0.5°C.

The water bulk temperature, T_w, was measured at a point well removed from all surfaces, and the vertical temperature distribution in the water was measured by using fixed thermocouples inserted through the test cell wall and by using a traversable needle probe. Due to the large temperature gradient which exists at the air–water interface, temperature measurements of the water in this region were also made using a rake of seven thermocouples installed 2.5 mm apart. Deionized water was used for all of the experiments, and the tests were performed under darkened laboratory conditions. The measurements were made no sooner than 2 h from the start of heating, after steady-state conditions were reached, and the Rayleigh number range associated with the experiments was $10^5 \lesssim Ra_D \lesssim 10^6$.

Flow visualization was implemented by using the thymol blue dye technique [8]. The negative electrode, which was a straight platinum wire of 0.076 mm diameter, was inserted in the region of the flow to be observed. By varying the electrode position, it was possible to observe boundary layer development around the cylinder and plume development above the cylinder.

EXPERIMENTAL RESULTS

Thymol blue was generated at two locations which are symmetrical about the bottom of a single heated cylinder, and representative results are shown in Fig. 2. Boundary layers develop on the cylinder, merge at the rear stagnation point, and form a buoyant plume which interacts with the air–water interface. From time-sequenced photographs taken after the start of thymol blue generation, the plume vertical velocity was estimated to be approximately 2 mm s^{-1} close to the cylinder surface and approximately 5 mm s^{-1} two cylinder diameters above the surface.

Plume and boundary layer conditions near the rear stagnation point are shown more clearly in Fig. 3. The photographs were taken at 20 s intervals, with thymol blue generated at the bottom and the upper right side of the cylinder. Two streamlines, which are close to the cylinder surface, rise on both sides of the cylinder and combine at the rear stagnation point to form a streamline at the midplane of the resulting two-dimensional plume. The other streamline, which originates at a point that is 4 mm from the cylinder surface, also moves toward the rear of the cylinder to form a

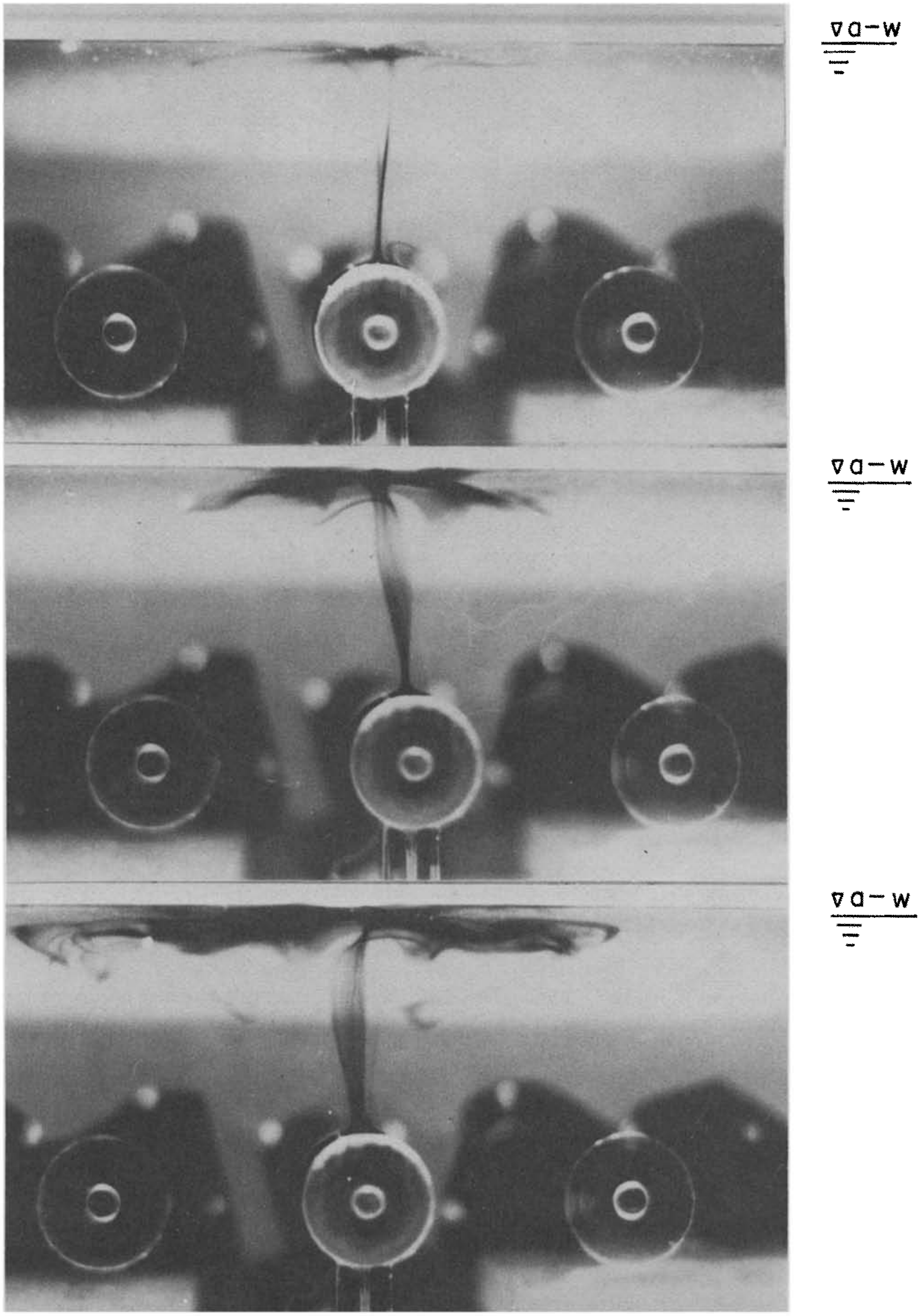

FIG. 2. Plume development and interaction with the air–water interface for a single heated cylinder ($Ra_D = 6.5 \times 10^5$, $H_1/D = 3.8$).

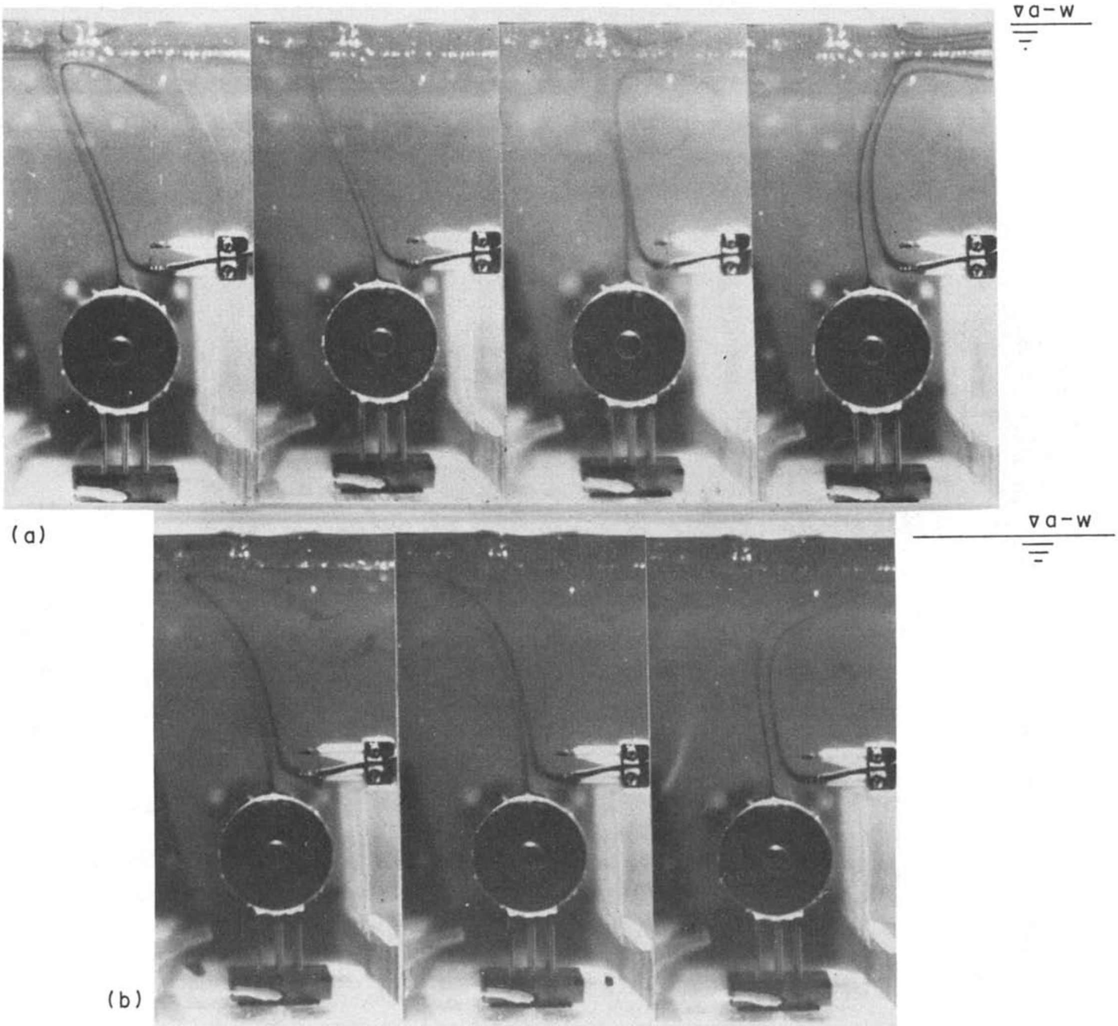

FIG. 3. Boundary layer and plume development for a single heated cylinder: (a) $Ra_D = 8.4 \times 10^5$, $H_1/D = 3.8$; (b) $Ra_D = 9.2 \times 10^5$, $H_1/D = 3.8$.

streamline at the periphery of the plume. This streamline indicates that the boundary layer is at least 4 mm thick near the top of the cylinder. It is evident that laminar flow conditions exist in both the boundary layer and the plume and that the boundary layer approaches the top of the cylinder without experiencing separation. This observation is consistent with the results of Pera and Gebhart [6]. The photographs also reveal that the flow is characterized by the regular swaying motion normally attributed to buoyant plumes [1, 2].

A comparison of Fig. 2, which is based on placement of the electrode assembly 27 mm from the cylinder end wall, and Fig. 3, which is based on placement of the assembly at the cylinder midplane, indicates the influence which the wall can have on plume motion. In Fig. 2 the neutrally buoyant tracer, which is 25 mm long, reveals an axial twisting or billowing which may be attributed to entrainment effects. The results also indicate that the amplitude of the plume oscillation is reduced near the wall. No such effects are revealed by the tracers of Fig. 3, which are well removed from the wall.

The nature of the plume interaction with the air–water interface is shown in Fig. 4. Upon deflection by the interface, the plume spreads horizontally, forming a layer of warm water which entrains cooler water from the underlying bulk fluid. In combination with heat losses across the air–water interface, the entrainment process causes the plume to cool as it spreads. The horizontal plume motion along the interface is characterized by turbulent mixing and an irregular vortex pattern. Vortex rings, which are generated in the plume mixing layer and may penetrate into the underlying fluid, are associated with the diffusion of large scale, low frequency turbulence. This diffusion of vorticity from the turbulent layer is shown most clearly in Fig. 4(b). It has also been observed by Shlien [9], and it resembles the penetrating convection process described by Turner [10]. However, the

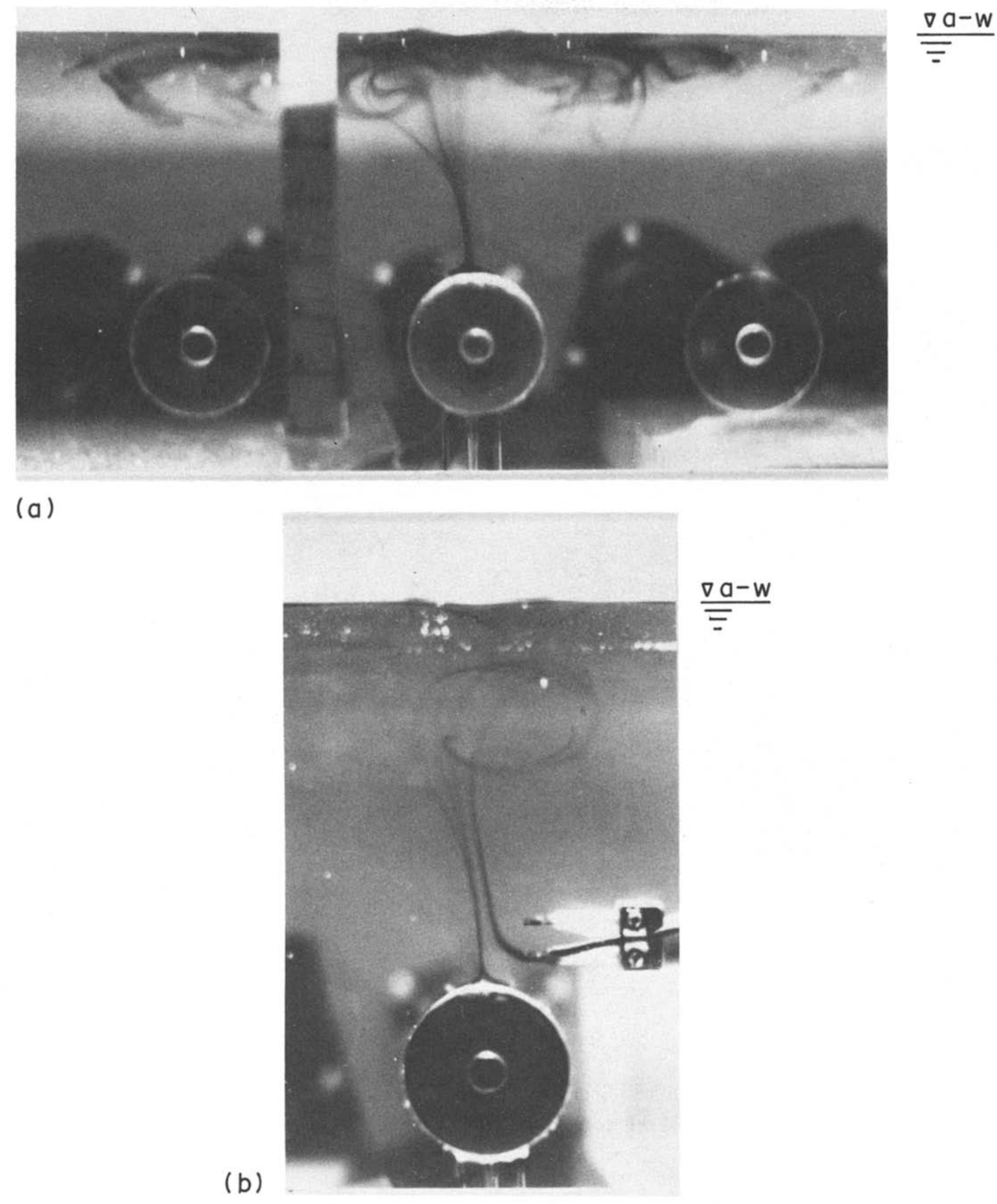

FIG. 4. Conditions in the plume mixing layer above a single heated cylinder ($Ra_D = 9.0 \times 10^5$, $H_1/D = 3.8$).

plunging sheets, which have also been observed for evaporatively cooled surface layers [11, 12], were not detected.

Plume behavior is a strong function of the height ratio, H_1/D, and results are shown in Fig. 5 for ratios of 3.8 and 2.5. The amplitude and period of the plume oscillation decreases with decreasing height ratio, and for $(H_1/D) \lesssim 2.5$, the oscillation is barely perceptible. Moreover, for $(H_1/D) \lesssim 2.5$ there is no longer any turbulent mixing or vortex ring formation. Instead, following a slight downward deflection, the plume moves horizontally in an ordered, streamline fashion.

Flow conditions have been observed for the array of heated cylinders, and the results of Fig. 6 were obtained with thymol blue generated at the middle three cylinders. For the prescribed conditions ($Ra_D = 4 \times 10^5$ and $H_1/D = 3.3$) each plume rises to the air–water interface, where it spreads horizontally. However, the plume motion does not continue to the side wall; instead adjoining plumes interact to establish a recirculating flow region. In this region fluid, which has partially cooled due to heat transfer from the air–water interface, descends to approximately the level of the cylinders, where it resumes a horizontal

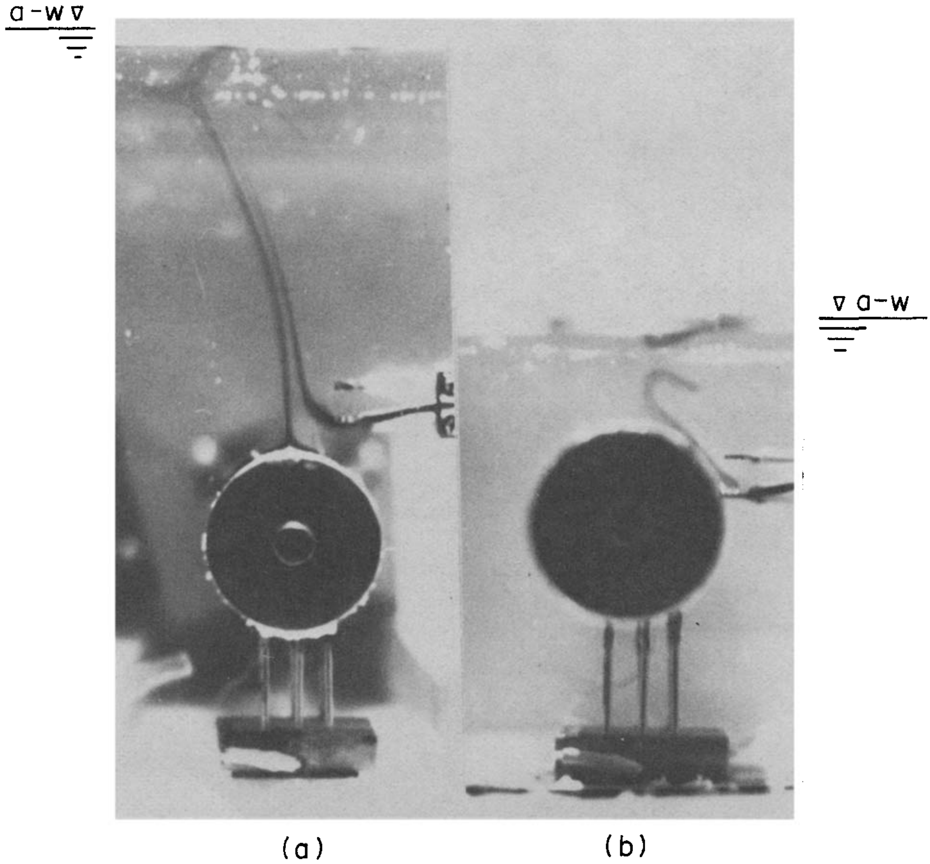

FIG. 5. Effect of height ratio on plume behavior: (a) $Ra_D = 9.2 \times 10^5$, $H_1/D = 3.8$; (b) $Ra_D = 6.4 \times 10^5$, $H_1/D = 2.5$.

motion. The recirculating flow can penetrate to the sides of the cylinder and interact with the free convection boundary layer. The net effect is one of subdividing the fluid above the cylinders into equivalent regions (cells) of recirculating flow. Note that, although plume oscillations still exist, their amplitude is greatly reduced.

The changes which begin to occur with increasing height ratio are shown in Figs. 7 and 8, which corresponds to $(H_1/D) = 4$ and $(H_1/D) = 5$, respectively. The magnitude of the plume oscillation increases with increasing height ratio, thereby increasing the probability of mutual plume interactions occurring below the air–water interface. The flow resulting from such interactions may take different forms. In Fig. 7(a), for example, two plumes originating from adjoining cylinders combine to form a single ascending plume; while in Fig. 7(b) a bifurcation

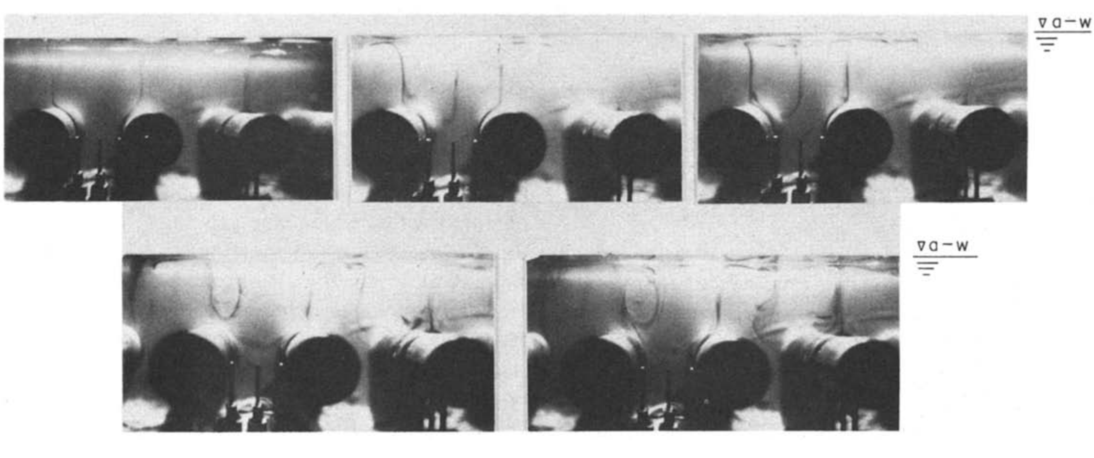

FIG. 6. Plume development and interaction for the array of heated cylinders ($Ra_D = 4 \times 10^5$, $H_1/D = 3.3$).

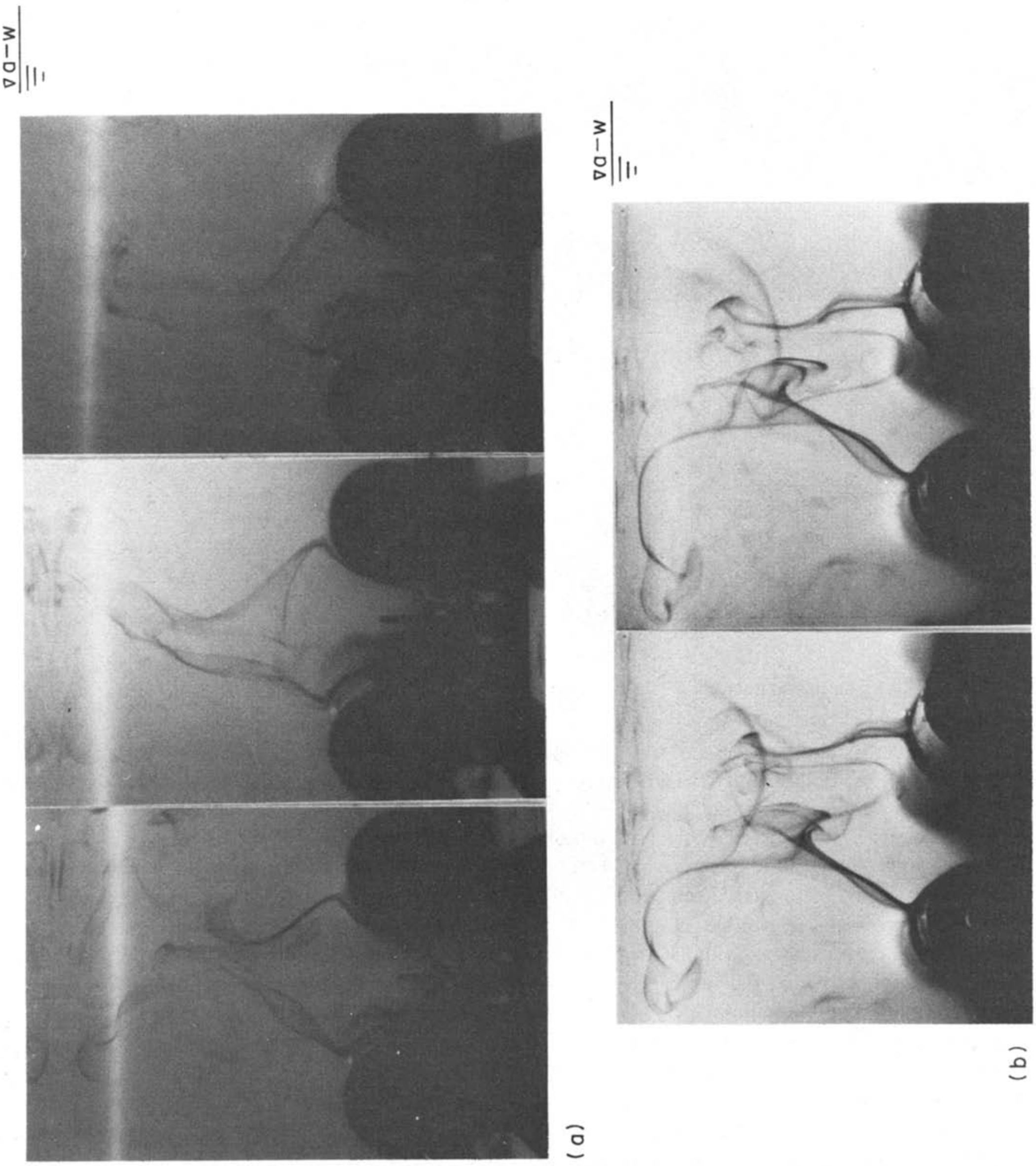

FIG. 7. Plume interactions for the array of heated cylinders ($Ra_D = 1.7 \times 10^5$, $H_1/D = 4$): (a) Ascending flow; (b) ascending and descending flows.

occurs which results in ascending and descending flows. In contrast flow resulting from the plume interactions may be highly disordered (Fig. 8) and characterized by many recirculating regions of varying size. The situation may also be such that some of the plumes are interacting, while others are rising to the interface.

Delineation of conditions in the test cell is facilitated by knowledge of the thermal structure. The vertical temperature distribution for the single cylinder was previously reported [13], and the results were characterized by a large unstable temperature gradient within the first 5 mm of the air–water interface. This condition has been observed by others [5, 12, 14], and the region has been termed a thermal boundary layer. It may be divided into a very thin surface layer, which is approximately 0.2 mm thick and in which heat transfer is dominated by diffusion, and a sublayer in which there exists some turbulent mixing. The adjoining plume mixing layer, which is 10–20 mm thick, is characterized by a slightly unstable temperature gradient, and the underlying bulk fluid is nearly isothermal.

The thermal structure has been resolved in more detail for the array, and representative results are shown in Figs. 9 and 10. The temperature distributions in Fig. 9 were obtained for two different Rayleigh numbers, using fixed thermocouples arranged on a vertical line which was midway between the outer cylinder and the test cell wall. The results of Fig. 10

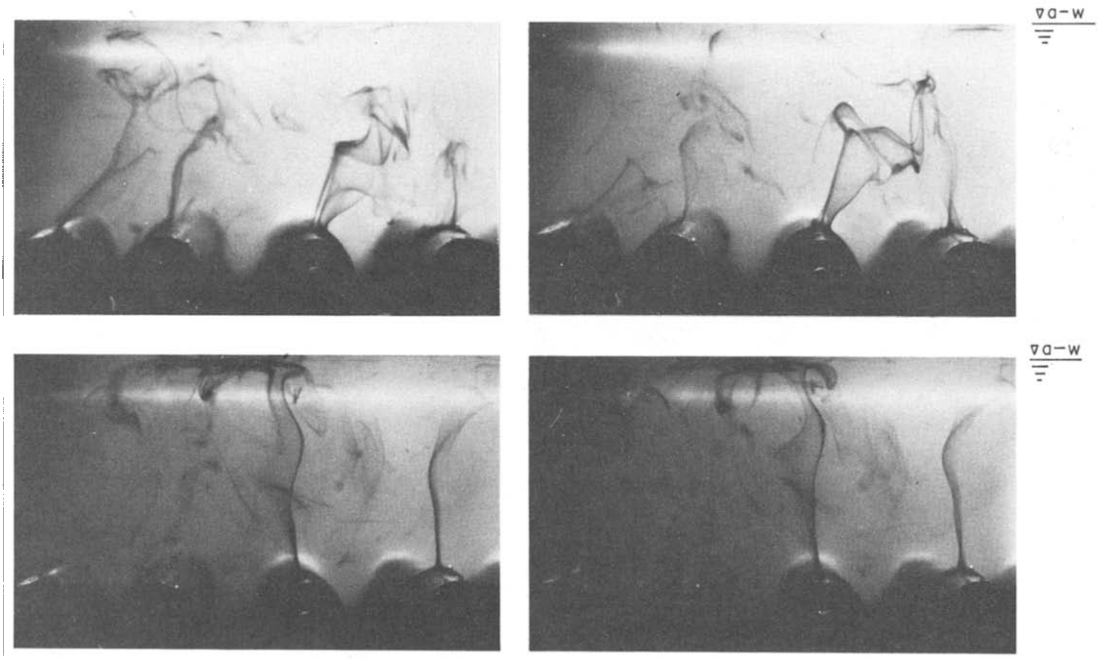

FIG. 8. Plume interactions for the array of heated cylinders (Ra_D = 1.9 × 10^5, H_1/D = 5).

pertain to a single Rayleigh number and were obtained using a traversable probe inserted between cylinders or between the outer cylinder and the cell wall.

As shown in Fig. 10, the water layer may be divided into four regions. The thermal boundary layer is characterized by a large, unstable temperature gradient. It consists of a very thin sublayer at the surface, in which the temperature distribution is linear, and an adjoining sublayer, in which the temperature distribution is approximately exponential. The temperature distribution in the thermal boundary layer is compatible with the existence of convective instabilities inferred from the flow visualization.

In the plume mixing layer, which is dominated by the interaction of plumes with each other and with the interface, temperature gradients remain large and the temperature reaches a maximum. This maximum has also been observed by Chang and Wagner [15] and attributed to convective instabilities induced by the unstable density gradient in the thermal layer. Its existence was confirmed for all space ratios and Rayleigh numbers of this study.

From the bottom of the plume mixing layer to a

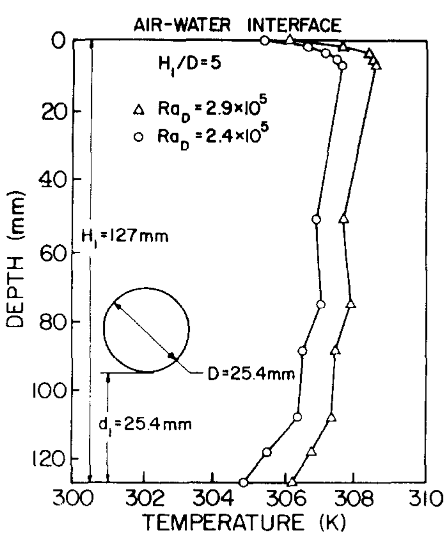

FIG. 9. Vertical temperature distribution between an outer cylinder and the side wall for an array of submerged heated cylinders (H_1/D = 5).

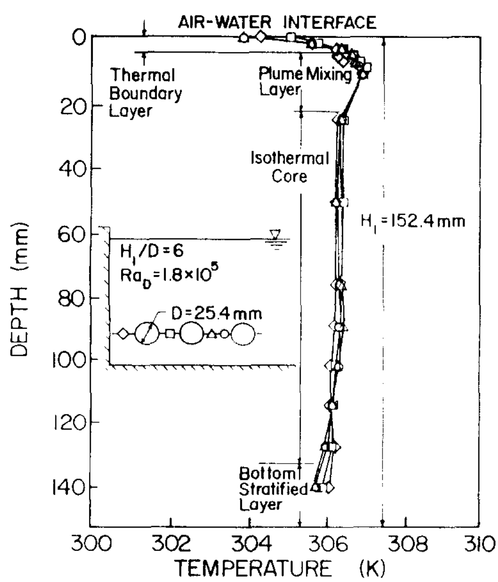

FIG. 10. Vertical temperature distributions between cylinders for an array of submerged heated cylinders (H_1/D = 6).

position just below the cylinders, the thermal structure is characterized by a nearly isothermal core. Conditions in this region are dominated by plume mixing effects, which contribute to maintaining a nearly uniform temperature. Stably stratified conditions exist in a region which extends from a point which is approximately 8 mm ($D/3$) below the bottom of the cylinders to the bottom of the test cell. The existence of a stable temperature distribution (Fig. 9) is consistent with the fact that no fluid motion was observed in this region.

Although plume deflections and interactions are known to increase with increasing height ratio, this effect has no influence on the general nature of the temperature distribution. The only variation is in the relative sizes of the four regions. For the smallest space ratio considered ($H_1/D = 3$), the boundary and plume mixing layers occupy most of the region above the cylinders, while the isothermal core is confined to a region which is slightly in excess of one cylinder diameter. For the largest height ratio ($H_1/D = 15$), however, there is little change in the extent of the boundary and plume mixing layers, and the isothermal core extends over most of the test cell. For all height ratios considered the bottom stratified layer has a thickness of approximately one cylinder diameter.

SUMMARY

The major conclusions of the study are summarized as follows.

(1) Laminar flow conditions exist in the cylinder boundary layer and in the plume which develops above the cylinder. Boundary layer merger occurs at the top of the cylinder without separation, and the boundary layer thickness and plume width in this region are at least 4 mm.

(2) The plume rising above a single cylinder exhibits the regular swaying motion normally attributed to buoyant plumes, and the amplitude and period of the oscillation increase with increasing height ratio.

(3) For the single cylinder and a height ratio (H_1/D) $\gtrsim 2.5$, interaction of the plume with the air–water interface results in a surface mixing layer which is approximately 20 mm thick and in which cooling occurs due to heat transfer across the interface and the entrainment of underlying fluid. Turbulent mixing in this layer is characterized by the formation of vortex rings which penetrate into the underlying fluid.

(4) Plumes generated by an array of cylinders interact in different ways. For (H_1/D) $\lesssim 4$, plume interactions occur at the air–water interface, and equivalent regions of recirculating flow are established between cylinders (Fig. 6). For (H_1/D) $\gtrsim 4$, however, the plumes may interact before reaching the interface to form a single ascending flow or a combination of ascending and descending flows. The interactions may also result in a highly disordered flow characterized by many recirculating regions of varying size.

(5) The vertical thermal structure is characterized by a surface thermal boundary layer having a large unstable temperature gradient, a mixing layer in which there is a temperature inversion, an isothermal core, and a stratified bottom layer in which there is a stable temperature gradient.

REFERENCES

1. R. J. Forstrom and E. M. Sparrow, Experiments on the buoyant plume above a heated horizontal wire, *Int. J. Heat Mass Transfer* **10**, 321–331 (1967).
2. T. Fujii, I. Morioka and H. Uehara, Buoyant plume above a horizontal line heat source, *Int. J. Heat Mass Transfer* **16**, 755–768 (1973).
3. J. Lieberman and B. Gebhart, Interactions in natural convection from an array of heated elements, experimental, *Int. J. Heat Mass Transfer* **12**, 1385–1396 (1969).
4. L. Pera and B. Gebhart, Laminar plume interactions, *J. Fluid Mech.* **68** (2), 259–271 (1975).
5. R. G. S. Skipper, J. S. C. Holt and O. A. Saunders, Natural convection in viscous oils, *International Developments in Heat Transfer*, Part V, pp. 1003–1010. ASME, New York (1961).
6. L. Pera and B. Gebhart, Experimental observations of wake formation over cylindrical surfaces in natural convection flows, *Int. J. Heat Mass Transfer* **15**, 175–177 (1972).
7. R. Eichorn, J. H. Lienhard and C. C. Chen, Natural convection from isothermal spheres and cylinders immersed in a stratified fluid, *Proc. 5th International Heat Transfer Conf.*, Tokyo, Japan, NC 1.3, pp. 10–14 (1974).
8. D. J. Baker, A technique for the precise measurement of small fluid velocities, *J. Fluid Mech.* **26** (3), 573–575 (1966).
9. D. J. Shlien, Some laminar thermal and plume experiments, *Phys. Fluids* **19**, 1089–1094 (1976).
10. J. S. Turner, *Buoyancy Effects in Fluids*. The University Press, Cambridge (1973).
11. W. G. Spangenberg and W. R. Rowland, Convection circulation in water induced by evaporative cooling, *Phys. Fluids* **4**, 747–750 (1961).
12. R. Viskanta, M. Behnia and A. Karalis, Interferometric observations of the temperature structure in water cooled or heated from above, *Adv. Water Resources* **1**, 57–69 (1977).
13. M. A. Yaghoubi and F. P. Incropera, Natural convection from a heated horizontal cylinder submerged in a shallow water layer, *Proc. 6th International Heat Transfer Conf.* Toronto, Canada, NC-15, pp. 269–274 (1978).
14. K. B. Katsaros, W. T. Liu, J. A. Businger and J. E. Tillman, Heat transport and thermal structure in the interfacial boundary layer measured in an open tank of water in turbulent free convection, *J. Fluid Mech.* **83** (2), 311–335 (1977).
15. J. H. Chang and R. N. Wagner, Laboratory measurement of surface temperature fluctuations induced by small amplitude surface waves, *J. Geophys. Res.* **80**, 2677–2686 (1975).

ECOULEMENTS DE CONVECTION NATURELLE AUTOUR DE CYLINDRES CHAUDS ET IMMERGES DANS UNE COUCHE D'EAU

Résumé – Des visualisations d'écoulement et des mesures de température permettent l'étude des couches d'eau peu profondes, chauffées en bas par des sources cylindriques et refroidies au dessus par l'interface d'air. Des expériences correspondent à un seul cylindre horizontal et à une rangée de cinq cylindres, avec des nombres de Rayleigh variant de 10^5 à 10^6. La couche limite de convection naturelle qui se développe sur le cylindre est laminaire et il n'y a pas de décollement au sommet du cylindre. Bien que le panache qui s'élève au dessus du cylindre unique est laminaire, son intéraction avec l'interface d'air produit une couche de mélange turbulent dans laquelle se forment des tourbillons annulaires qui pénètrent dans le fluide sous-jacent. L'intéraction des panaches formés par la rangée de cylindres prend différentes physionomies qui dépendent de la hauteur de la couche.

AUFTRIEBSSTRÖMUNGEN AN BEHEIZTEN ZYLINDERN IN EINER WASSERSCHICHT ENDLICHER DICKE

Zusammenfassung – Strömungs-Sichtbarmachung und Temperaturmessungen werden benutzt, um die Verhältnisse in flachen Wasserschichten zu untersuchen, die von unten durch zylindrische Wärmequellen beheizt und von oben an einer Luftoberfläche gekühlt werden. Es wurden Experimente für einen einzelnen horizontalen Zylinder und für eine Reihe von fünf Zylindern mit Rayleigh-Zahlen im Bereich von 10^5 bis 10^6 durchgeführt. Die Grenzschicht der freien Konvektion, die an den Zylindern entsteht, ist laminar, und eine Vereinigung der Grenzschicht erfolgt an der Oberseite der Zylinder ohne Ablösung. Obwohl der Streifen, der über dem einzelnen Zylinder aufsteigt, laminar ist, erzeugt seine Wechselwirkung mit der Luftoberfläche eine horizontal turbulent durchmischte Schicht, in der sich Wirbelringe bilden und in die darunterliegende Flüssigkeit eindringen. Die Wechselwirkung der Streifen, die durch die Zylinderreihe erzeugt werden, tritt je nach Höhenverhältnis in unterschiedlicher Form in Erscheinung.

СВОБОДНОКОНВЕКТИВНЫЕ ПОТОКИ, ВОЗНИКАЮЩИЕ НА НАГРЕВАЕМЫХ ЦИЛИНДРАХ, ПОГРУЖЕННЫХ В СЛОЙ ВОДЫ КОНЕЧНОЙ ТОЛЩИНЫ

Аннотация — С помощью визуализации течения и измерения температур исследовались условия в слоях воды небольшой толщины, нагреваемых снизу цилиндрическими источникам и охлаждаемых сверху воздушной границей раздела. Эксперименты проводились с единичным горизонтальным цилиндром и с системой из пяти цилиндров при изменении числа Релея в диапазоне от 10^5 до 10^6. Свободноконвективный пограничный слой, развивающийся на цилиндрах, носил ламинарный характер, а слияние пограничных слоёв происходило в верхней части цилиндров без отрыва. Несмотря на то, что поднимающаяся над единичным цилиндром струя имеет ламинарный характер, её взаимодействие с воздухом на границе раздела приводит к образованию горизонтального турбулентного слоя смешения, в котором образуются вихревые кольца, проникающие в нижележащие слои жидкости. Взаимодействие струй, генерируемых системой цилиндров, происходит иным образом и зависит от отношения высот.